sustainability

Article

Simulation-Based Optimization of the Urban Thermal Environment through Local Climate Zones Reorganization in Changsha City, China with the FLUS Model

Jie Chen [1], Ruijie Shi [1], Geng Sun [1], Ya Guo [1], Min Deng [1] and Xiuyuan Zhang [2,*]

[1] School of Geosciences and Info-Physics, Central South University, Changsha 410083, China; cj2011@csu.edu.cn (J.C.); 205011045@csu.edu.cn (R.S.); 215007004@csu.edu.cn (G.S.); guoyaa@csu.edu.cn (Y.G.); dengmin@csu.edu.cn (M.D.)
[2] School of Earth and Space Sciences, Peking University, Beijing 100871, China
* Correspondence: xy_zhang@pku.edu.cn

Abstract: Urbanization leads to changes in surface landscapes, such as the increase in built-up areas and the decrease in natural elements, resulting in local changes in land surface temperature, which often create unusually hot weather and affect livability, especially for mid- and low-latitude cities. Therefore, optimizing urban landscapes and adjusting the thermal environment is especially important to improve comfort and to achieve sustainable urban development. Existing studies on optimizing landscapes have considered mainly horizontal land uses/land covers but ignored their elevation. This study considered local climate zones as basic units to describe three-dimensional landscapes; we measured the relationship between local climate zones and land surface temperature, based on which the research further used a genetic algorithm and future land-use simulation models to optimize the spatial layouts of local climate zones in Changsha, China, considering multiple objectives including adjusting land surface temperature without affecting population carrying capacity, economic development, watershed protection, and forest and grass protection. According to the optimization results, the area of open low-rise buildings increased by 5.98% after optimization, and dense trees decreased by 7.64%; open low-rise buildings were suggested to be newly built in the city center and sparsely buildings should be developed in the surrounding administrative district far away from the city center. The optimization results contributed to a −5.2 °C reduction of average land surface temperature, which could significantly improve the thermal environment under the premise of ensuring the population and economic development levels and thus serves as a novel solution for improving urban landscapes to implement sustainable city development.

Keywords: land surface temperature; WUDAPT; three-dimensional landscape; urbanization; sustainable development

Citation: Chen, J.; Shi, R.; Sun, G.; Guo, Y.; Deng, M.; Zhang, X. Simulation-Based Optimization of the Urban Thermal Environment through Local Climate Zones Reorganization in Changsha City, China with the FLUS Model. *Sustainability* **2023**, *15*, 12312. https://doi.org/10.3390/su151612312

Academic Editor: Miguel Amado

Received: 28 June 2023
Revised: 29 July 2023
Accepted: 3 August 2023
Published: 12 August 2023

1. Introduction

“The 2030 Agenda for Sustainable Development” adopted by the United Nations aims to achieve peace, prosperity, and development for humanity and the planet; for urban development; and for sustainable development. It requires the construction of safe, livable, and sustainable cities and human settlements [1,2]. Urban land is the basic carrier of social and economic development and also the main scene of environmental pollution and ecological damage. How to utilize urban land scientifically and efficiently, considering the limited natural resource endowment, is crucial to promote sustainable urban development.

In recent years, urbanization has changed land uses/land covers (LULC), where built-up land has increased, and green areas have decreased, and these changes have led to changes in urban heat environments [3–5]: (1) The increase in artificial coverage types such as buildings and roads leads to the increase in surface reflectivity and the rise in urban land surface temperature (LST); (2) tall buildings block ventilation corridors, making it difficult to diffuse thermal energy, dense building clusters form air barriers that block air convection, and heat is conducted in the form of turbulence, leading to the production of urban heat islands; (3) the reduction of natural-cover types such as vegetation and water lead to changes in the water–air environment, evaporation is reduced, and the heat is difficult to transform, which increases the urban LST; and (4) the urban population and socio-economic activities also produce heat [6,7]. Different LULC often correspond to different socio-economic activities, thus generating heat and leading to an increase in the urban heat island effect. Global extreme weather (such as extremely hot days) is abnormal, seriously affecting the quality of life of urban residents and hindering urban sustainable development. Thus, urbanization has led to a spatially-heterogeneous increase in the urban LST and a decrease in the comfort of the urban environment.

The spatial optimization of landscapes can influence the LST; thus, it is the key to improving the natural environment and implementing sustainable city development. The Chinese government has paid great attention to the spatial pattern of urban LULC and has been working hard in recent years to build livable cities. Therefore, it is important to optimize landscapes to improve urban ecological environments and livability. The existing research on landscape optimization mainly involves the optimal allocation of LULC. Early LULC optimization mainly considered indicators directly related to land resources, such as the land utilization rate, land revenue, land compactness, and land development costs [8,9]. With attention to ecological environments, some studies were conducted to optimize land use from an ecological perspective by considering the ecological effects of land uses [10,11]. In addition to ecological effects, LULC optimization has multiple impacts on habitability, and thus some studies have considered optimization models with multiple constraints. For example, the Basic Agricultural Land and Ecological Red Line [12] were used as constraints when performing LULC optimization, and the influence of social, economic, and natural factors on LULC optimization could be considered simultaneously as objectives [13]. There were also some studies introducing various socio-economic indicators to simulate and optimize the spatial patterns of LULC [14,15]. However, the above-mentioned studies only considered spatial optimization of LULC layout under single scenarios, and LULC optimization involves multiple scenarios, such as natural development scenarios and sustainable development scenarios, which require the establishment of multi-scenario land-use models to simulate the changes and spatial patterns of LULC under different scenarios [14,16]. In setting spatial optimization objectives, most studies considered maximizing the compactness of cities as a target [17], and such an objective ensures the compactness of urban LULC. With a focus on sustainable development, the optimization goals of many studies have been to enhance ecosystem service value (ESV), which is important for human health, livelihoods, and survival [18]. In addition, more research has focused on the evaluation of the sustainable development status of land uses [19,20], and the optimization of urban layouts of production–life–ecological space based on the goal of coordinating spatial patterns and functional uses [21–23].

Although existing studies have provided very valuable research ideas and methods, there are also problems. Firstly, previous research focused on two-dimensional LULC, and most of the studies focused on evaluations of the current situation of LULC as well as their spatial patterns [8,9]. Few studies considered height information of buildings and vegetation and did not optimize urban LULC from a three-dimensional perspective. Secondly, the optimization objectives also mostly considered the ecological value impacts brought by land uses, but did not consider the urban heat environment and urban suitability [14,15]. The urban LST is an important indicator of human settlement suitability, and it is not only related to the type of land cover, but it is also related to three-dimensional city morphology and land patterns such as the height and density of buildings and green areas [24]. Accordingly, previous studies are weak in understanding the influence of complex city morphology on the spatial heterogeneity of LST using a three-dimensional perspective; thus, an external and independent classification system for urban areas that is different from LULC and helpful for urban LST studies is needed, and local climate zones (LCZs) [25] can be a potential solution.

LCZs were proposed by Stewart and Oke [25], which provided an external and standardized classification protocol for urban climate studies. LCZs are composed of areas with the same ground cover structure, material, and human activities; 17 types are defined based on the physical characteristics of the urban environment. Recent research has shown that this classification can be used to study the influence of city morphology on LST [16,26] and heat environmental comfort [27,28]. LCZ optimization can improve the urban heat environment in a more efficient way, which can achieve both the optimization of the urban natural ecological environment and the sustainable development of the social population and economy, and it can provide a new perspective for improving the urban heat environment. However, no studies have optimized LCZs for improving the urban heat environment.

Each LCZ type has different land-cover types, different albedos, different row forms, and different sub-bedding surfaces [25]. The definition of LCZs also includes attributes such as sky openness, cover height and density, and building materials [29,30]. These attributes are correlated with the LST, which reflects the urban heat environment. High temperature often corresponds to the built-up area, and natural covers of LCZs can reduce the LST [31,32]. The attributes of LCZs also reflect the living and productive activities of humans. For example, the population represents the attraction and social development of a city, and a dense population is often closely associated with high-density buildings; GDP reflects the economic development level of a city, and areas with high GDP are often associated with tall buildings [33,34]. Therefore, urban landscape optimization should consider the above built, environmental, and socio-economic influences.

As demonstrated above, LCZs can represent heterogeneous urban landscapes, and they can have impacts on the local LST, but there is little knowledge on how to adjust LCZs as well as their layouts to reduce the extreme heat of the LST and improve the thermal environment. To resolve this issue, we measured the multiple attributes of LCZs with climate, socioeconomic, and LCZ datasets, the used genetic algorithm (GA), and the future land-use simulation (FLUS) model to optimize LCZs. The GA considers making the urban LST as close as possible to the human comfort temperature under the premise of ensuring the city's population carrying capacity and smooth economic development. It is mainly used to optimize the quantity structure of LCZs to meet the requirements of sustainable development and government policies. Furthermore, based on the optimization result of GA, the FLUS model is used to optimize the spatial layout of LCZs, which is applied to Changsha, one of the "Stove Cities" in China. The study generally makes three contributions to the field of knowledge: (1) measuring LCZ impacts on temperature, population, and economy, which is essentially a reference for the optimization of LCZs to improve living environments; (2) generating advice for creating a more comfortable living environment; and (3) giving reasonable spatial land-pattern layouts for building a city with livable temperatures. The city directly contributes to environmental comfort improvement by optimizing spatial layouts of LCZs without affecting socio-economic development, which helps to implement sustainable city development.

2. Study Area

Changsha is located in central China, downstream of the Xiangjiang River and at the western edge of the Changliu Basin. It is a central city and an important logistics and transportation center of the Yangtze River. Changsha has a complex topography with large undulations. There are large mountains in the northeast and northwest with elevated terrain, while the central region is flat (Figure 1). Changsha has a subtropical monsoon climate, which is influenced by natural factors such as winter and summer monsoon transitions and the northward slope of the terrain, resulting in a rain–heat period and distinct seasons.

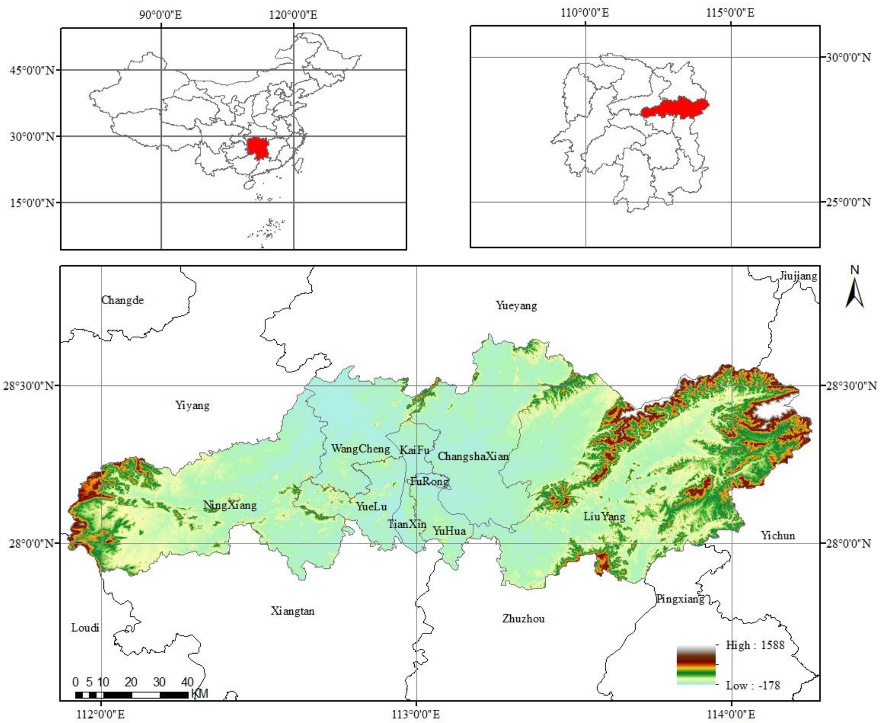

Figure 1. Location of the study area and DEM in 2020.

In recent years, Changsha has been developed rapidly, with an urban population increasing by about 56.04% and a built-up area increasing by about 85.26% between 2010 and 2020 [35]. The concentration of population and accelerated urbanization have also caused problems such as urban heat island and extreme heat. According to statistics from the meteorological department, in the summer season the average daily maximum temperature is over 29 °C. The hottest month of the year in Changsha is July, with an average maximum temperature of 32 °C and an average minimum temperature of 25 °C. There is almost no rain in the summer, and the absolute maximum temperature in the summer can reach 40 °C. There are 85 days with an average daily temperature over 30 °C, and 30 days of hot weather over 35 °C. Therefore, the thermal environment of Changsha is in critical need of being mitigated.

3. Materials and Methods

3.1. Datasets and Preprocessing

The main data in this paper are climate and socioeconomic datasets related to urban thermal environment and remote sensing data used for LCZ classification. The climate and socioeconomic datasets include population, GDP, LST, and building height. The remote sensing data include Landsat 8 images, and the specific data sources are shown in Table 1. After acquiring all data, we used ArcGIS10.2 software to pre-process the data. All data coordinate systems were converted to GCS_WGS_1984_UTM_Zone_ 50 N. Since the spatial resolution of all raster data images was 1 km × 1 km except Landsat, we used a 1 km × 1 km grid to unify all data.

Table 1. Data and sources.

Data	Source	Time	Description
Population	Landscan Website https://landscan.ornl.gov/ (accessed on 20 February 2023)	2010, 2015, 2020	The resolution of the raster data is 1 km; data are used to count the dynamic distribution of the global population.
GDP	Resource and Environment Science and Data Center https://www.resdc.cn/ (accessed on 20 February 2023)	2010, 2015, 2020	The resolution of the raster data is 1 km; these data are generated by spatial interpolation of the gridded data based on national GDP statistics.
LCZs	Landsat 8 OLI	2010, 2015, 2020	LCZ classification was performed on the WUDAPT platform using Landsat 8 OLI raster data with a resolution of 30 m.
LST	Terra MODIS	2010, 2015, 2020	The LST raster data are inverted by Terra MODIS data and include daytime and nighttime data. The spatial resolution is 1 km, and the temporal resolution is 8 days. The mean value of the raster is used to represent the LST for the corresponding year.
Building height	Geographic Remote Sensing Ecological Website https://www.gisrs.cn/ (accessed on 20 February 2023)	2020	City building outline and building height vector data; building height is from the floor of the building.

3.2. Research Framework

This work aims to optimize urban LST and provides suggestions for improving urban suitability. The framework mainly includes the following steps: (1) LCZ classification and correlation analysis using the World Urban Database and Access Portal Tool (WUDAPT) [29] to classify the LCZs in the study area with 30 m × 30 m Landsat 8 remote sensing images; make urban LST, population, and GDP distribution maps; analyze the spatial distribution characteristics of LCZs and multi-factors; and analyze the correlation between LCZs and multi-factors. (2) Establishing optimization objective and constraints: Combining the distribution characteristics of LCZs and the distribution characteristics of LST, population, and GDP in the study area, the optimization objective is determined to control the urban LST within the comfortable temperature range of humans. Moreover, the area of water bodies, forest and grass coverage, and population carrying capacity are considered; GDP level and total land area are used as constraints; and the genetic algorithm is employed to optimize the quantitative structure of urban LCZs, and dynamically simulate the changes of the LCZ spatial layout through intrinsic driving factors and conversion costs. (3) Spatial simulation of optimization results: Based on the LCZs of Changsha in 2020, a GA-FLUS model is established to optimize the LCZs of Changsha city, suggesting an overall optimization plan and providing development suggestions for Changsha (Figure 2).

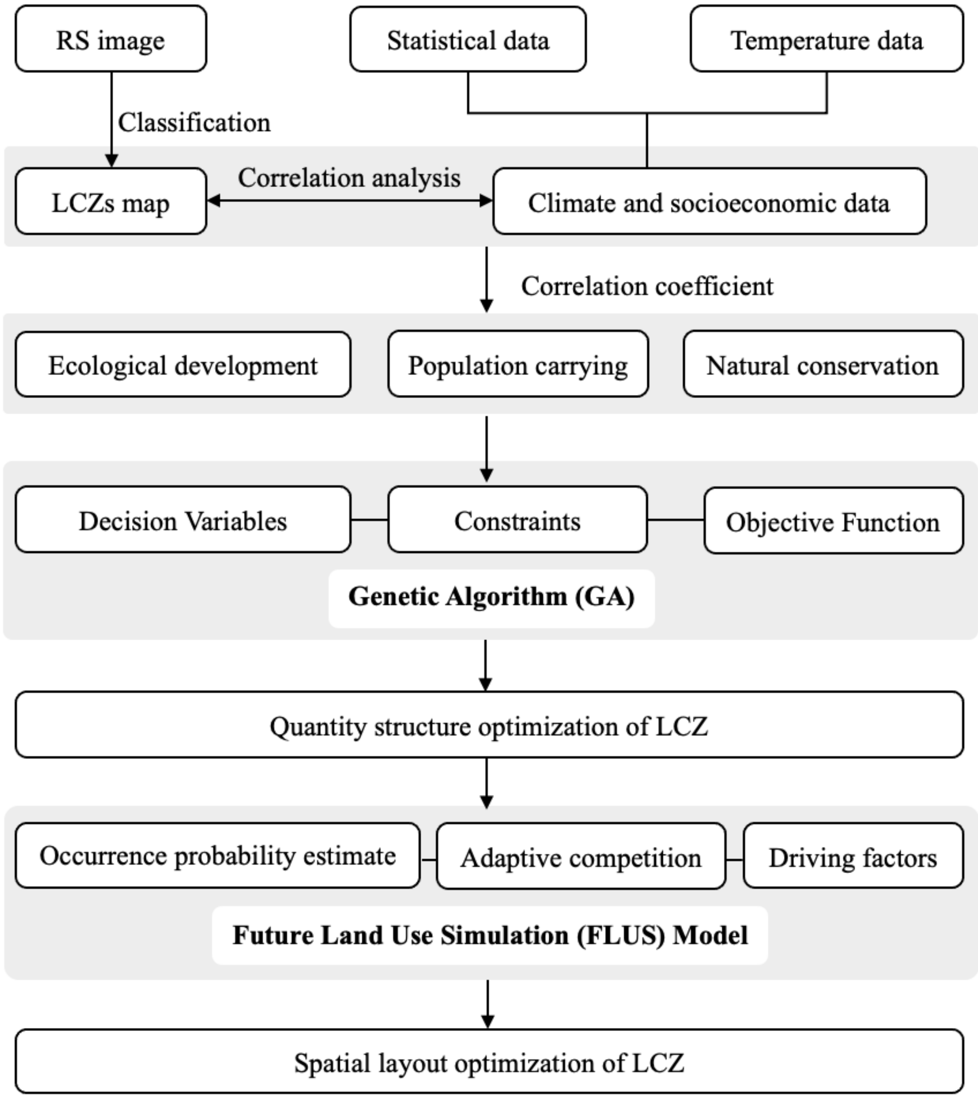

Figure 2. Research framework.

3.3. LCZ Classification

This study used the WUDAPT for LCZ classification. The WUDAPT provides instructions for LCZ classification with open-access data and open-source software. This approach has achieved significant results in several countries and regions. According to the WUDAPT classification method developed by Bechtel [29], it can be broadly divided into four steps: Landsat satellite data preparation, digitization of the training area in Google Earth, classification in SAGAGIS, and validation of the results and redefinition of the training area.

Firstly, we downloaded and preprocessed 30 m resolution Landsat satellite images of Changsha from USGS and resampled the images to 300 m in SAGAGIS to obtain the spectral signal of local-scale urban features. Secondly, we employed vectorization by Google Earth to achieve polygonized representative areas of each LCZ as training areas. Each LCZ included 20–30 training samples. Table 2 shows the examples of LCZs. The selected LCZ training samples were the same as the LCZs. Thirdly, we loaded the preprocessed Landsat satellite images and selected training samples for SAGAGIS classification, using Random Forest to classify the LCZs in the study area according to the similarity of the training samples and the rest of the study area. The LCZs were then mapped. Finally, we considered a validation and training area redefinition, and we exported the KML file from the generated LCZ map and loaded it into Google Earth for validation. We then resampled the inconsistent training area and repeated the last step until it was consistent with the actual situation. Furthermore, the confusion matrix, Kappa coefficient, and overall accuracy were obtained using the Confusion Matrix tool of SAGA GIS to estimate the LCZ classification accuracy. When the Kappa coefficient and overall accuracy were both larger than 0.7, the LCZ classification results were considered to be acceptable.

Table 2. The definition and examples of local climate zones [25].

LCZs	**LCZ1 Compact High-Rise Buildings**	**LCZ2 Compact Mid-Rise Buildings**	**LCZ3 Compact Low-Rise Buildings**
Definition	Dense mix of tall buildings (average height over 25 m). Few or no trees. Land cover mostly paved. Concrete, steel, stone, and glass construction materials.	Dense mix of mid-rise buildings (average height 10–25 m). Few or no trees. Land cover mostly paved. Stone, brick, tile, and concrete construction materials.	Dense mix of low-rise buildings (average height 3–10 m). Few or no trees. Land cover mostly paved. Stone, brick, tile, and concrete construction materials.
LCZ examples	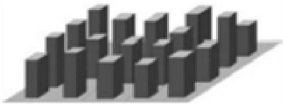		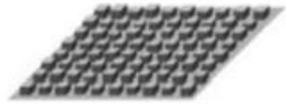
Image examples			
LCZs	LCZ4 Open high-rise buildings	LCZ5 Open mid-rise buildings	LCZ6 Open low-rise buildings
Definitions	Open arrangement of tall buildings (average height over 25 m). Abundance of pervious land cover (low plants, scattered trees). Concrete, steel, stone, and glass construction materials.	Open arrangement of mid-rise buildings (average height 10–25 m). Abundance of pervious land cover (low plants, scattered trees). Concrete, steel, stone, and glass construction materials.	Open arrangement of low-rise buildings (average height 3–10 m). Abundance of pervious land cover (low plants, scattered trees). Wood, brick, stone, tile, and concrete construction materials.
LCZ examples		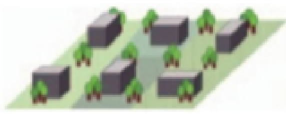	
Image examples			

Table 2. *Cont.*

LCZs	LCZ1 Compact High-Rise Buildings	LCZ2 Compact Mid-Rise Buildings	LCZ3 Compact Low-Rise Buildings
LCZs	LCZ7 Lightweight low-rise	LCZ8 Large low-rise buildings	LCZ9 Sparse buildings
Definitions	Dense mix of single-story buildings. Few or no trees. Land cover mostly hard-packed. Lightweight construction materials.	Open arrangement of large low-rise buildings (lower than 10 m). Few or no trees. Land cover mostly paved. Steel, concrete, metal, and stone construction materials.	Sparse arrangement of small- or medium-sized buildings in a natural setting. Abundance of pervious land cover (low plants, scattered trees).
LCZ examples		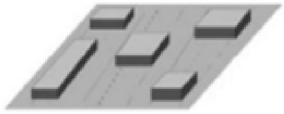	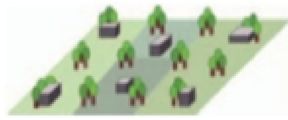
Image examples			
LCZs	LCZ10 Heavy industries	LCZ11 Dense trees	LCZ12 Scattered trees
Definitions	Low-rise and mid-rise industrial structures (towers, tanks, stacks). Few or no trees. Land cover mostly paved or hard-packed. Metal, steel, and concrete construction materials.	Heavily wooded landscape of deciduous and/or evergreen trees. Land cover mostly pervious (low plants).	Lightly wooded landscape of deciduous and/or evergreen trees. Land cover mostly pervious (low plants).
LCZ examples	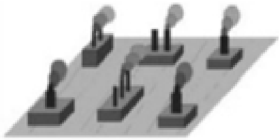		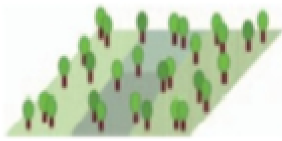
Image examples			
LCZs	LCZ13 Brush and scrub	LCZ14 Low plants	LCZ15 Bare rock or road
Definitions	Open arrangement of bushes; shrubs; and short, woody trees.	Featureless landscape of grass or herbaceous plants/crops. Few or no trees.	Rock or paved cover. Few or no trees or plants.
LCZ examples	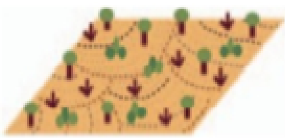		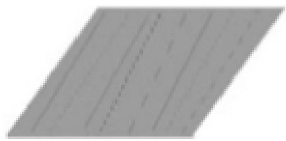
Image examples			

Table 2. *Cont.*

LCZs	**LCZ1 Compact High-Rise Buildings**	**LCZ2 Compact Mid-Rise Buildings**	**LCZ3 Compact Low-Rise Buildings**
LCZs	LCZ16 Bare soil or sand	LCZ17 Water	
Definitions	Soil or sand cover. Few or no trees or plants.	Large, open water bodies.	
LCZ examples	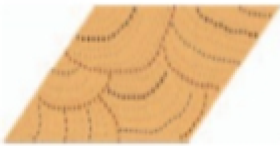		
Image examples			

3.4. LCZ Layout on the Expression of Multifactorial Action Relationship

Urban LST is not only related to land cover, but it is also influenced by urban morphology, population activities, and production activities. Therefore, it is important to establish the relationships between LCZs and LSST, population, and economy for urban spatial optimization. Different LCZs have different contributions to urban socio, economic, and natural factors. Furthermore, the grid analysis method can connect different spatial resolution data, which is convenient for statistics and analysis data. The spatial location of the grid is fixed, and the grid size can be set to be flexible, thus allowing for easy analysis of multiple datasets. In this paper, we used a total of 12,421 regular grids of 1000 $\times$ 1000 to integrate the LCZ map, LST, population distribution, and GDP grid. The average values of LCZ temperature, population, and GDP were obtained by taking the maximum values of LCZ classification maps and the average values of LST, population, and GDP data in the same grid cell.

Based on the grid analysis, we explored the influence of the number of different LCZ types on urban socio, economic, and natural factors, and we used the area ratio of different LCZ types in the 1000 m grid to represent the number of LCZs. We analyzed their relationship with temperature, population, and GDP and quantitatively analyzed the correlation between LCZs and socio, economic, and natural factors. We use ArcGIS for analysis. Firstly, we chose the Identify Tool of Spatial Overlay Analysis to connect the 1000 m grids with LCZ classification results. Then, the Frequency Tool of Statistical Analysis was used to count the area of each LCZ type in each grid and calculate the area ratio of each type of LCZ using the same method to count the average values of LST, population, and GDP in each grid. Finally, the average LST, population, and GDP values of different LCZ types under different proportions were counted at 10% area ratio intervals, and the statistical results were regressed and analyzed to obtain the linear equations of correlation between each type of LCZ and temperature, population, and GDP.

3.5. Optimization of LCZ Area Ratio

LCZ area ratio optimization is a complex problem with great uncertainty because the LCZs contain the natural states of land covers and multiple attributes of population, temperature, and economic levels associated with human activities, and the area ratios of the LCZs need to consider the constraints and effects of various attributes. There are two main types of methods for solving LULC-optimization problems: exact methods and heuristic methods [36]. Exact methods evaluate all feasible solutions and find a unique set of non-dominated solutions. The application of exact methods in LULC-optimization problems is limited because it is a complex optimization that not only optimizes the number of each plot type but also their spatial layout. Many studies have shown that exact methods are effective when the targets are simple and constraints are not conflicting [37]. However, in the real world, urban spatial optimization problems are always conflicting. When the optimization problem is simple, the exact method shows good performance. However, due to the many factors of urban spatial layout and the complexity of the optimization problem, the exact method is not the best choice when solving the LULC-optimization problem. In contrast to exact methods, heuristic methods use rules of thumb or best practices to produce a set of near-optimal solutions. Research results have shown that the most commonly used heuristic algorithm for solving LULC-optimization problems is the genetic algorithm [36].

The genetic algorithm is an algorithm that solves global optimization, and its basic principle is to simulate biological evolutionary processes such as natural selection, heredity, and mutation by continuously evolving the population so as to continuously approach the optimal solution. By setting decision variables, objective functions and constraints, the fitness calculation, selection calculation, crossover operation, and variation operation are performed. The fitness calculation is used to measure the fitness value of each individual, and the individual with higher fitness is considered as the better solution. The selection calculation is a probabilistic selection based on the fitness value of an individual to select the better individual to ensure that good genes are inherited. The crossover operation is conducted to cross over the genomes of two individuals in some crossover manner to generate a new individual. The mutation operation is conducted to randomly mutate some genes of an individual to ensure the diversity of the population and prevent it from falling into a local optimal solution. After iterations, the optimized individuals will keep approaching the optimal solution. The algorithm can be used for the optimization of the LCZ area ratio, and the genetic algorithm has outstanding advantages compared to other optimization algorithms. Firstly, the algorithm is difficult to disturb through changes in external conditions during operation, and it is suitable for the optimization of complex systems. Secondly, the genetic algorithm is an algorithm that focuses on the set of individuals, and it has large-scale computing power and parallel search capability. Thirdly, the genetic algorithm follows the natural-selection process to achieve global optimization, which can ensure that LCZs conform to the rules of natural development and reach the optimal goal to the greatest extent. In this study, we hope to establish the LCZ area ratio optimization model with the goal of improving the urban LST based on the correlation between LCZs and socio-economic natural factors so as to provide the urban spatial layout scheme with livable temperatures for human beings. The genetic algorithm construction process of this study is as follows:

3.5.1. Selection of Decision Variables

The decision variables are the base part of the genetic algorithm, and the selection of decision variables will be different according to different optimization purposes. The selection of decision variables should be consistent with the classification results of LCZs, which can reflect the natural-cover state of LULC and also the future development direction of LULC. In this paper, 17 decision variables were established based on the LCZ classification results of Changsha, which represent 17 types of LCZs.

3.5.2. Construction of the Objective Function

In order to improve the urban heat environment and provide suitable living environmental temperatures for human beings, consistent with urban sustainable development planning requirements, the optimization goal is to control the LST within the comfort range of the human body's surface temperature (22–26 °C), i.e.,

$$22 \le \left(LST = \sum_{i=1}^{I} W \times X_i \right) \le 26 \quad (1)$$

where *LST* represents the land surface temperature, *W* is the average temperature coefficient per unit area of each LCZ, X_i represents the area of each type of LCZ, and i indicates the LCZ type (taking values 1–17).

3.5.3. Construction of Constraints

The construction of constraints is a key step in model optimization, which involves the limitation of the range of model results. In this paper, five constraints were mainly considered, as shown in Table 3: watershed protection, forest and grass cover, population, socio-economy, and land area.

Table 3. The constraint conditions of the optimization model.

	Formula	Meaning	Interpretation
Watershed Protection	$X_{17} \geq A_{water}$	According to the urban water development plan, the urban water area should not be less than that in the base year.	Where X_{17} represents the area of the water body after optimization, and A_{water} represents the total area of the water body in the city's base year.
Forest and Grass Cover	$\frac{(X_{11}+X_{12}+X_{13}+X_{14})}{\sum_{i=1}^{I} X_i} \geq FRG$	To prevent urban erosion, the forest and grass cover must not be lower than the current value.	Where X_{11}, X_{12}, X_{13}, X_{14} represent the urban forest and grassland cover area after optimization, and FRG represents the forest and grassland cover of the base year.
Population	$\sum_{i=1}^{7} M \times X_i \geq P$	To protect people's livelihoods, the city's population should be no smaller than the current population.	Where M is the average population carrying capacity per unit area of each LCZ, X_1–X_7 is the area of the building type after optimization, and P represents the total urban population in the base year.
Socio-Economy	$\sum_{i=1}^{I} G \times X_i \geq E$	In order to ensure the development of the city's economy, the city's GDP should not be smaller than the current GDP.	Where G is the average GDP per unit area of each LCZ, X_i is the area of each type of LCZ after optimization, and E represents the urban GDP in the base year.
Land Area	$\sum_{i=1}^{I} X_i = A_{total}$	The sum of all types of LCZ area is the total LULC area.	Where X_i is the LCZ area of each type after optimization. A_{total} denotes the total land area of Changsha.

3.6. Optimization of Spatial LCZ Layout

The spatial layout optimization of LULC has experienced long-term development. The main methods include Markov models [38], cellular automata models (CA) [39], land change models [40], land use and impact transformation models [41], etc. Due to the complexity and uncertainty of land, these approaches did not consider the intrinsic drivers of land use change, such as geography, economy, energy, resources, society, and policy, resulting in inconsistencies between land use change and legal change.

The future land use simulation (FLUS) model is a model to simulate land change and land scenarios under the influence of human activities and the natural environment, which can reveal the potential drivers of land change and combine land expansion analysis strategies with the cellular automata (CA) model to better simulate the evolution of multiple land patches in space and time. The model was proposed by Liu [17] considering multiple natural- and human-driven factors, and adaptive inertia and competition mechanisms are employed in the modeling process. The study also developed the FLUS model as free downloadable and usable software (GeoSOS-FLUS 2.0.0a). The applications in several cities also have achieved significant results, proving the advantages of the FLUS model in simulating land use change [42,43]. The FLUS model is a dynamic simulation model; it is important for learning nonlinear land use change, and its simulation accuracy is higher than other traditional models. Combining the optimized geospatial model (GeoSOS) and the future land use model (FLUS) can simulate LULC spatial change scenarios under the influence of natural and human activities and provide a reference for spatial layout optimization. The model calculates the probability of occurrence of various types of LCZs based on the data of various driving factors using a neural network, and then it sets the neighborhood factors, inertia coefficient, and conversion cost and combines them with the probability of occurrence to calculate the conversion probability of LCZs. Then, the complexity and uncertainty of urban land area are simulated and optimized by using roulette wheel selection, and the optimization results are obtained.

3.6.1. Estimate the Probability of Occurrence of LCZs

Artificial neural network (ANN) is a machine learning model developed based on biological neural networks. It includes a series of neurons and layers with some ability to learn complex relationships between input data and training objects. In the GeoSOS-FLUS model, we chose social, economic, ecological, and environmental data as driving factors. Then, these factors were combined by the ANN model to calculate the probability of occurrence of each LCZ type in each pixel.

The ANN model consists of an input layer, a hidden layer, and an output layer, and the neurons in the input layer correspond to the LCZs of each plot and are calculated as

$$X(k,t) = [x_1(k,t), x_2(k,t), x_3(k,t), \ldots, x_n(k,t)]^T \tag{2}$$

where $x_i(k,t)$ is the i-th variable associated with input neuron i in grid unit k at time t, and T is the transformation.

Neuron j in the hidden layer receives the signal net j (k, t) in grid k from the input layer at time t and is calculated as

$$net_j(k,t) = \sum_i w_{ij} x_i(k,t) \tag{3}$$

where w_{ij} is the adaptive weight of input layer i to hidden layer j. The response function of the receiving neuron j in the hidden layer is called the activation function.

In order to obtain a more accurate LCZ type, a random perturbation term is also added when calculating the probability of occurrence. The final occurrence probability is calculated as

$$\mathrm{P(k,t,z)} = \left[1 + (-\ln rand)^{\beta}\right] \times \sum_j w_{j,z} \frac{1}{1 + e^{-net_j(k,t)}} \tag{4}$$

where $\mathrm{P(k,t,z)}$ is the probability of plot conversion to class z, rand is a random variable from 0 to 1, and β is a parameter that controls the fluctuation of the random variable.

3.6.2. Adaptive Inertia Competition Mechanism

The probability of LCZ variation not only depends on the distribution probability of the neural network output but also on the neighborhood effect, inertia coefficient, and conversion cost.

A. Neighborhood effect: The probability of LCZ change is influenced by the type and number of LCZs in the neighborhood. There are two common types of neighborhoods: the Von Neumann neighborhood and the Moore neighborhood. The Von Neumann domain with a radius of 1 includes 4 cells around the target cell, and the Moore domain with a radius of 1 includes 8 cells around the target cell. In the spatial optimization of LCZs, we used the Moore neighborhood to represent the neighborhood range of LCZ cells and to consider the effect of the surrounding LCZs and number on the change probability of the target LCZ cells. The change probability is expressed as

$$\Omega_{p,k}^t = \frac{\sum_{N\times N} con\left(c_p^{t-1} = k\right)}{N \times N - 1} \times w_k \tag{5}$$

where N represents the number of neighborhoods, and w_k represents the influence coefficient of the neighborhoods.

B. Inertia coefficient: The inertia coefficient of each type of LCZ is determined by the gap between the current number of LCZs and the target number of LCZs, and it is adaptively adjusted in the iterations so that the number of LCZs of each type gradually approaches the target number in the simulation process.

$$Intertia_k^t = \begin{cases} Intertia_k^{t-1} & if \left| D_k^{t-1} \right| \leq \left| D_k^{t-2} \right| \\ Intertia_k^{t-1} \times \frac{D_k^{t-2}}{D_k^{t-1}} & if D_k^{t-1} < D_k^{t-2} < 0 \\ Intertia_k^{t-1} \times \frac{D_k^{t-1}}{D_k^{t-2}} & if 0 < D_k^{t-2} < D_k^{t-1} \end{cases} \quad (6)$$

where $Intertia_k^t$ denotes the inertia coefficient of the kth LCZ at iteration time t, D_k^{t-1} and D_k^{t-2} denote the difference between the pixel number of the kth LCZ and the number required at iteration time $t-1$ and $t-2$, respectively.

C. Conversion cost: The difficulty of converting different LCZ types to other LCZ types is different and is usually represented by a conversion-cost matrix. The range of the conversion cost is [0, 1], and higher values mean a more difficult and costly conversion [44,45]. In our study, the development planning needs of Changsha were considered, and the conversion costs of various types of LCZs are shown in Table 4 after integrating Balling's and Liu's study on the conversion costs of land use types. In order to protect the water body, we specified that the water body cannot be converted to any other type of LCZ. Building types are more difficult to convert to natural-cover types, and building types can be converted to each other, but the conversion cost is higher for dense buildings. The conversion cost of each LCZ type is shown in Table 4.

Table 4. The conversion costs of local climate zones.

LCZs	1	2	3	4	5	6	8	9	10	11	12	13	14	15	16	17
1	0	0.7	0.6	0.7	0.6	0.5	0.6	0.7	0.8	0.9	0.8	0.7	0.9	0.8	0.9	1
2	0.5	0	0.6	0.7	0.6	0.5	0.6	0.7	0.8	0.9	0.8	0.7	0.9	0.8	0.9	1
3	0.5	0.7	0	0.7	0.6	0.5	0.5	0.7	0.8	0.9	0.8	0.7	0.9	0.8	0.9	1
4	0.5	0.6	0.5	0	0.7	0.4	0.5	0.5	0.7	0.8	0.7	0.6	0.8	0.7	0.9	1
5	0.8	0.6	0.5	0.6	0	0.4	0.5	0.5	0.7	0.8	0.7	0.6	0.8	0.7	0.9	1
6	0.8	0.6	0.5	0.6	0.7	0	0.5	0.5	0.7	0.8	0.7	0.6	0.8	0.7	0.9	1
8	0.8	0.6	0.5	0.6	0.5	0.4	0	0.5	0.6	0.8	0.7	0.6	0.8	0.7	0.9	1
9	0.8	0.7	0.5	0.6	0.5	0.4	0.6	0	0.6	0.8	0.7	0.6	0.8	0.7	0.9	1
10	0.8	0.7	0.5	0.6	0.7	0.4	0.6	0.7	0	0.8	0.7	0.8	0.8	0.7	0.9	1
11	0.9	0.8	0.8	0.7	0.7	0.6	0.7	0.4	0.8	0	0.5	0.6	0.6	0.5	0.8	0.9
12	0.9	0.8	0.8	0.7	0.7	0.6	0.7	0.4	0.8	0.4	0	0.6	0.6	0.5	0.8	0.9
13	0.9	0.8	0.8	0.7	0.7	0.6	0.7	0.4	0.8	0.4	0.5	0	0.6	0.5	0.8	0.9
14	0.9	0.8	0.8	0.7	0.7	0.6	0.7	0.3	0.7	0.4	0.5	0.5	0	0.5	0.8	0.9
15	0.8	0.7	0.7	0.6	0.6	0.4	0.5	0.5	0.5	0.5	0.7	0.6	0.8	0	0.8	0.9
16	0.8	0.7	0.7	0.6	0.6	0.4	0.5	0.5	0.5	0.5	0.7	0.5	0.6	0.4	0	0.9
17	1	1	1	1	1	1	1	1	1	1	1	1	1	1	1	0

Considering the influence of occurrence probability, neighborhood effect, inertia coefficient, and conversion cost, the total probability of each LCZ conversion can be expressed as

$$Prob_{n,k}^t = P(k,t,z) \times \Omega_{n,k}^t \times inertia_k^t \times (1 - sc_{c \to k}) \quad (7)$$

where $Prob_{n,k}^t$ represents the total probability of conversion of class k LCZs at iteration time t, $P(k,t,z)$ represents the estimated probability based on ANN, $\Omega_{n,k}^t$ represents the probability of LCZ change at iteration time t under the influence of the neighborhood, $inertia_k^t$ represents the inertia coefficient of class k LCZs, $sc_{c \to k}$ represents the conversion difficulty of LCZ conversion from class c to class k, and $1 - sc_{c \to k}$ represents the probability of LCZ conversion from class c to class k. Furthermore, the LCZ conversion cost matrix (Table 4) was developed in combination with Balling's research [34]. The transfer matrix considers not only of the conversion difficulty of LCZs but also the watershed protection and forest land protection policies. It can be applicable to most cities in China. However, the conversion cost matrix can also be fine-tuned for each city's special situation.

3.6.3. Roulette Wheel Selection

Considering the competition between LCZs, in roulette wheel selection, the LCZ type with the highest combination probability is the most likely to transform, but other LCZ types with low combination probabilities may also transform. We introduce "fitness" and "cumulative probability", where the probability of each component being selected is proportional to its fitness value, calculated as follows:

$$\mathrm{P}\left(x_i = \frac{f(x_i)}{\sum_{j=1}^{i} f_j}\right) \quad Q(x_i) = \sum_{j=1}^{i} P(x_i) \tag{8}$$

where x_i represents the class i LCZ, the fitness value of x_i is $f(x_i)$, the probability of being selected is $P(x_i)$, and the cumulative probability is $Q(x_i)$.

The cumulative probability represents the sum of the probability of all choices of each LCZ, which is equivalent to the "span" on the roulette wheel; the larger "span" is more likely to be chosen. The process of roulette wheel selection is as follows: (1) Calculate the probability of each individual being selected ($P(x_i)$); (2) calculate the cumulative probability, $Q(x_i)$, of each part; (3) randomly generate an array m, with the elements of the array taking values between 0 and 1, and sort them from smallest to largest. If the cumulative probability, $Q(x_i)$, is greater than the element mi in the array, the individual is selected, and if it is less than mi, the next individual is compared until an individual is selected.

4. Results and Discussion

4.1. LCZs and Multifactor Correlation Analysis

4.1.1. LCZ Classification

Figure 3 shows the LCZ classification results of Changsha. Sixteen types of LCZs were identified in the study area, including nine built-up types and seven natural-cover types, and Table 5 shows the corresponding land types of each LCZ. On the whole, the LCZs of built-up types were mainly distributed in the center of the city. For example, the area adjacent to the Xiangjiang River and YueLu District is a cluster of open mid-rise buildings (LCZ5), where the terrain was flat and the scenery beautiful and suitable for human habitation. The urban center at the junction of TianXin District, FuRong District, and KaiFu District east of the Xiangjiang River had a large number of compact high-rise buildings (LCZ1), which are the administrative districts of Changsha. The edges of the five main administrative districts of TianXin, YuHua, FuRong, KaiFu, and YueLu were mainly large low-rise buildings (LCZ8), and then there were open low-rise buildings (LCZ6) in the surrounding areas, which had good infrastructure, were close to the city center, and were the main places for human habitation and living. Natural-cover LCZ types were mainly distributed in the east and northwest alpine areas, such as the western part of NingXiang and the eastern part of LiuYang, with a large number of dense trees (LCZ11), where the terrain is high and the landform types are complex, with the famous Xiangshan Mountain and Dawei Mountain Forest Park; sparse buildings (LCZ9) were also present in a high proportion in NingXiang and LiuYang, accompanied by natural-cover types of LCZs. In addition, water (LCZ17) was mainly distributed in the area where the Xiangjiang River flowed through. According to Table 6, the area of dense trees (LCZ11) in the whole Changsha area had the largest proportion, reaching 43.85%. Combined with the map of LCZ classification results in Changsha, it can be seen that Changsha had a large number of natural-cover resources, which were distributed in the east and west of the city. Among the building types, the area of sparse buildings (LCZ9) had the largest proportion at 28.93% and was scattered around the city along with natural-cover types. Compact high-rise buildings (LCZ1) had the highest average number of building floors with 12 floors, and heavy industries (LCZ10) had the lowest number of average building floors with 2 floors. The average number of building floors of each LCZ type generally conformed to the definition of LCZs.

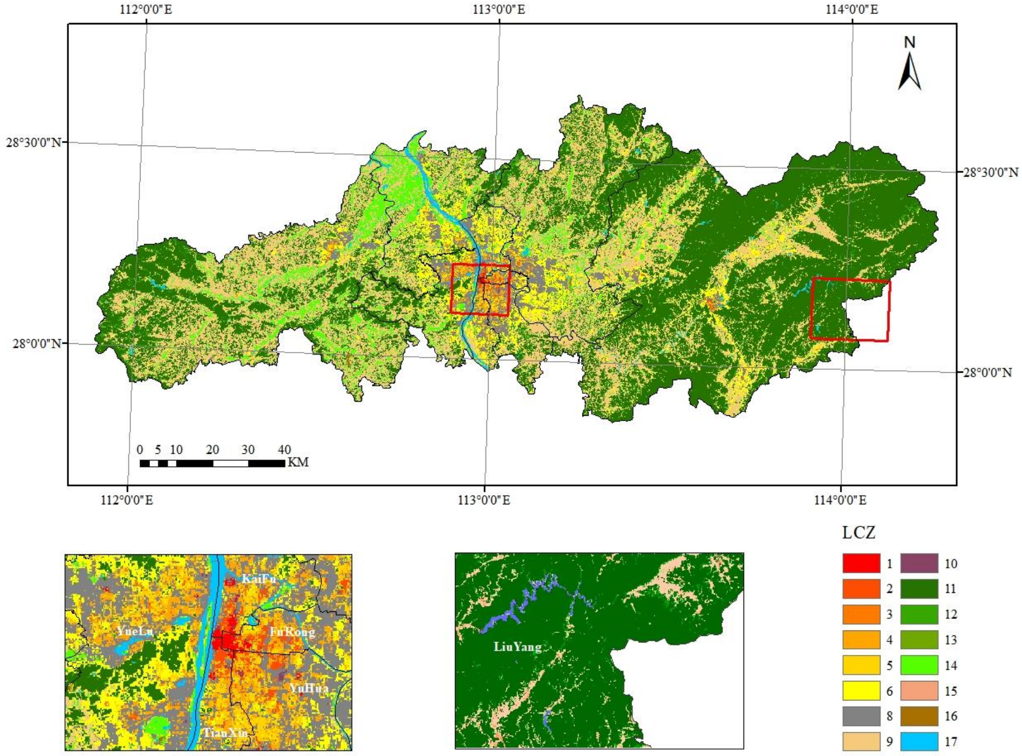

Figure 3. The local climate zones of Changsha in 2020.

Table 5. The corresponding land cover types of local climate zones.

Land Cover Types	LCZs	Land Cover Types	LCZs
Built-up	LCZ1 Compact high-rise LCZ2 Compact high-rise LCZ3 Compact high-rise LCZ4 Open high-rise LCZ5 Open high-rise LCZ6 Open low-rise LCZ8 Large low-rise LCZ9 Sparsely built LCZ10 Heavy industries	Natural vegetation cover	LCZ11 Dense trees LCZ12 Scattered trees LCZ13 Scattered trees LCZ14 Low plants
		Other natural land cover	LCZ15 Bare rock or paved LCZ16 Bare soil or sand
		Water	LCZ17 Water

Table 6. The area and mean height of local climate zones.

LCZs	Area Percentage	Average Floor	LCZs	Area Percentage
LCZ1 Compact high-rise	0.04%	12	LCZ11 Dense trees	43.85%
LCZ2 Compact high-rise	0.14%	7	LCZ12 Scattered trees	5.99%
LCZ3 Compact high-rise	0.19%	4	LCZ13 Scattered trees	0.002%
LCZ4 Open high-rise	0.64%	10	LCZ14 Low plants	6.66%
LCZ5 Open high-rise	0.72%	9	LCZ15 Bare rock or paved	0.04%
LCZ6 Open low-rise	7.78%	3	LCZ16 Bare soil or sand	0.10%
LCZ8 Large low-rise	3.62%	4	LCZ17 Water	1.27%
LCZ9 Sparsely built	28.93%	6		
LCZ10 Heavy industries	0.03%	2		

4.1.2. Spatial Distribution Patterns of LST, Population, and Economy from an LCZ Perspective

In this paper, we first used the grid analysis method to obtain the average value of LST, population, and GDP for each LCZs. Figure 4a shows the LST map of Changsha in 2020. The highest LST in Changsha in 2020 was 30.25 °C, and the lowest temperature was 14.35 °C. The maximum temperature was mainly concentrated in the central urban area, and the temperature gradually decreased from the central part to the surrounding area, with obvious heat island effects. Figure 4b shows the average LST of each type of LCZ in 2020. The average LST of the building type was generally higher than the LST of the natural-cover type. Among the built-up types, the average LST of compact mid-rise buildings (LCZ2) reached a maximum value of 30.2 °C, while the average LST of open low-rise buildings (LCZ6) had the lowest value at 24.91 °C. Overall, the average LST of the compact built-up type was higher than the LST of the open built-up type. Among the natural-cover types, the highest mean LST was 27.23 °C in rocks or roads (LCZ15), and the lowest mean LST was 21.65 °C in water (LCZ17). The average LST decreased with the increase in vegetation density. Combined with the results of LCZ classification in Changsha in 2020, it could be seen that the average LST was related to the LCZ type. Usually, in the denser buildings, worse ventilation was related to higher LST, so the average LST of dense buildings was higher than the LST of open buildings. Higher vegetation cover caused lower LST, so the LST of the natural-cover type was generally lower than that of the building type. The type and spatial distribution of LCZs had great influences on the LST. Thus, an optimal configuration of LCZs could help improve the urban thermal environment.

Figure 4c shows the average population in Changsha in 2020. The maximum population was 32,902/km^2, and the minimum population was 0/km^2. The population was concentrated in the central region, with minor human clusters in LiuYang and NingXiang. There were no population clusters in the dense forest at the edge of the city. Figure 4d shows the average population of each type of LCZ in Changsha in 2020. Furthermore, the average population of built-up types was generally more than that of natural-cover types. Among all built-up types, large low-rise buildings (LCZ8) had the largest average population of 1.31 million, while heavy industries (LCZ10) had the smallest average population. Among the natural-cover types, dense trees (LCZ11) had the largest average population of 537,500, while bush and scrub (LCZ13) had the smallest average population. Combined with the results of LCZ classification in Changsha in 2020, the average population of different categories of LCZ differed, and the distribution of population not only reflected the preferences of people's daily life activities but also was closely related to factors such as building density, ventilation, and natural environment. Compared with the dense built-up type, the population was more distributed in the open built-up type, which had more green area and good ventilation, and the open built-up type also had more public space, and humans could have more space for activities. The type and spatial distribution of LCZs had a great influence on the population, and the change of population needs to be considered when optimizing LCZs.

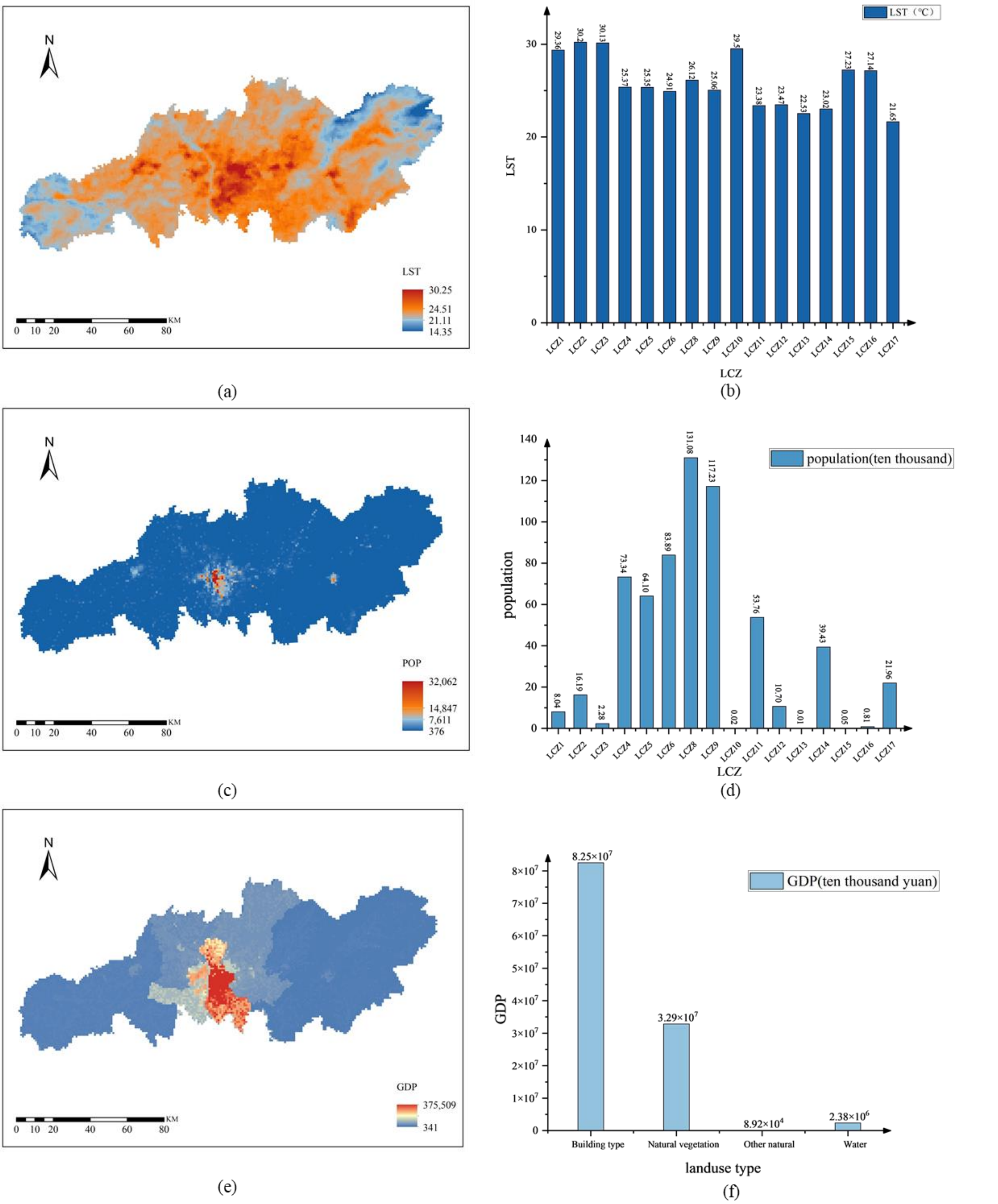

Figure 4. Spatial distribution patterns of land surface temperature, population, and economy from a local climate zones perspective. (**a**) The land surface temperature of Changsha in 2020; (**b**) the land surface temperature of each local climate zone; (**c**) the population of Changsha in 2020; (**d**) the population of each local climate zone; (**e**) the GDP of Changsha in 2020; (**f**) the GDP of each land use.

Figure 4e shows the average GDP in Changsha in 2020. The maximum value of the average GDP was CNY 375.509 million per km^2, and the minimum value was CNY 3.41 million per km^2. The high value of GDP was concentrated in the central region, decreasing in a block shape in all directions, and the dividing line was more obvious. The GDP was mainly affected by land use and national economic activities. The GDP generated by agriculture, forestry, animal husbandry, and fisheries corresponded to the type of land used for the corresponding purpose, where the GDP of agriculture, forestry, and animal husbandry were mainly generated on land naturally covered with vegetation, and the corresponding LCZs were LCZ11–LCZ14, while the GDP of fisheries was mainly generated on water-covered land, and the corresponding LCZ was LCZ17. The GDP related to human activities was mainly generated in the category of buildings and other naturally covered land, and the corresponding LCZs were LCZ1–LCZ10 and LCZ15LCZ16. The average GDP of each land type was obtained based on the average GDP of each LCZ type. Figure 4f shows the average GDP of each land type in 2020; the highest GDP was CNY 8.25×10^7 million for building types, and the lowest average GDP was CNY 8.92×10^4 million for other natural-cover types. Combined with the results of LCZ classification in Changsha in 2020, different categories of LCZs corresponded to different LULC with different GDP values, reflecting the economic efficiency of different LCZ types. In general, the average GDP of LCZs of building types was higher than that of the natural-cover type, which was because built-up areas are the main places of human production and living activities, and the economic activities are frequent. The LCZs and spatial distribution affected the change of GDP and also influenced social and economic development. Therefore, when optimizing LCZs, the impact of LCZ changes on GDP should be considered.

From qualitative analysis, we found that there was a certain connection between LCZs and LST, population, and GDP, and further correlation analysis was conducted for the number of LCZs and each factor. The average LST, average population, and average GDP of different numbers of different types of LCZs is shown in Figure 5. The correlation coefficients for Changsha City in 2020 are shown in Table 7:

Table 7. The correlation coefficients of Changsha in 2020. W is the correlation coefficient between the local climate zone area ratio and the average land surface temperature, M is the correlation coefficient between the local climate zone area ratio and the average population, and G is the correlation coefficient between the local climate zone area ratio and the average GDP.

LCZs	W	M	G
LCZ1 Compact high-rise	0.7977	2620	62,888.38
LCZ2 Compact high-rise	0.6829	1905.2	62,888.38
LCZ3 Compact high-rise	0.4337	1496.7	62,888.38
LCZ4 Open high-rise	−0.214	1328.8	62,888.38
LCZ5 Open high-rise	−0.3337	848.14	62,888.38
LCZ6 Open low-rise	−0.5294	112.23	62,888.38
LCZ8 Large low-rise	−0.4849	−63.314	62,888.38
LCZ9 Sparsely built	0.0703	31.97	62,888.38
LCZ10 Heavy industries	0.6457	24.4	62,888.38
LCZ11 Dense trees	−0.6191	−8.2	609.5
LCZ12 Scattered trees	−0.402	−9.9143	609.5
LCZ13 Scattered trees	−0.5249	−15.4	609.5
LCZ14 Low plants	−0.4286	−162.49	609.5
LCZ15 Bare rock or paved	0.4054	−1483.6	13,725.71
LCZ16 Bare soil or sand	0.3606	−320.31	13,725.71
LCZ17 Water	−0.7983	−411.77	−5262.6

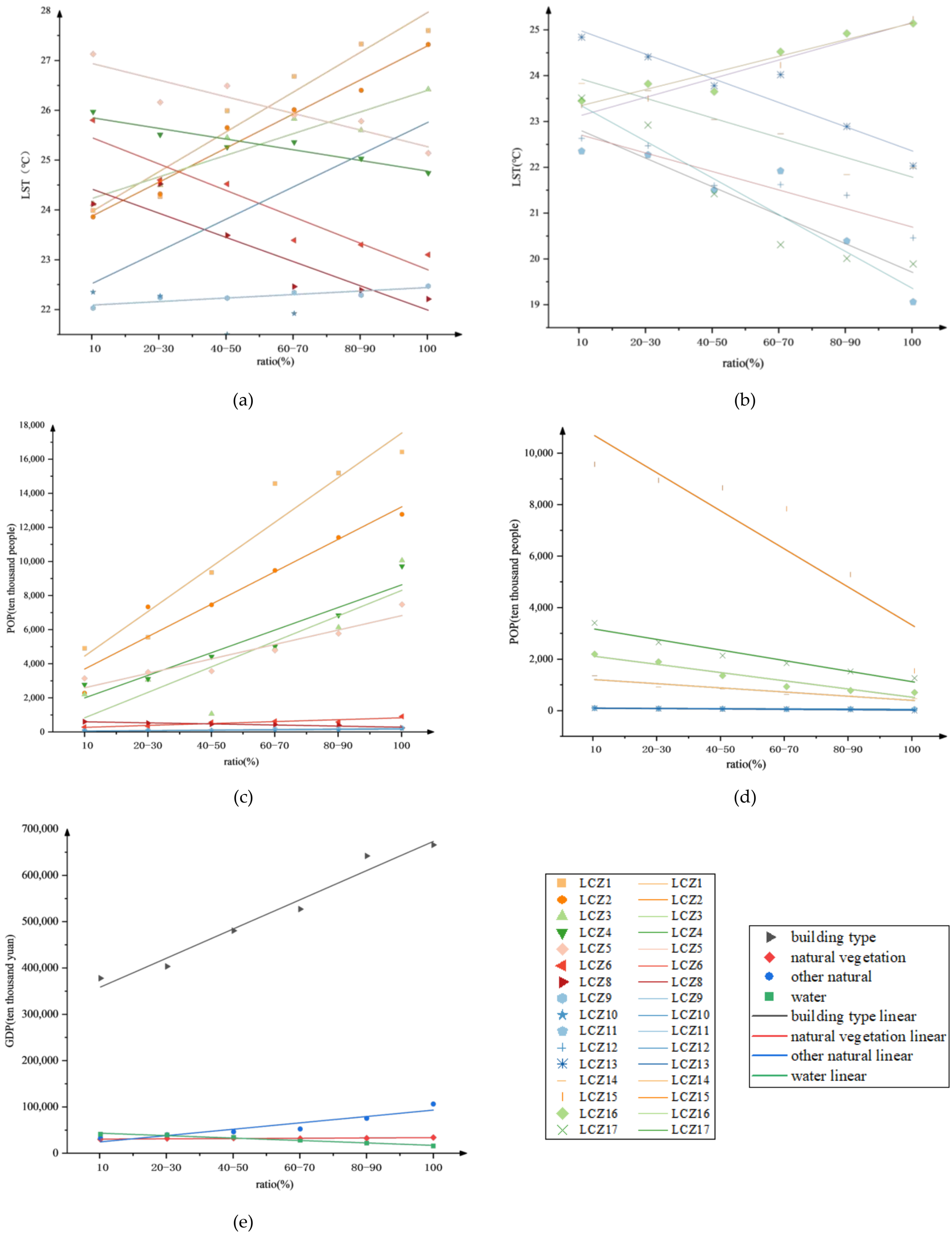

Figure 5. The correlation analysis. (**a**) Urban-type land surface temperature mean values in different ratios; (**b**) nature-type land surface temperature mean values in different ratios; (**c**) urban-type population mean values in different ratios; (**d**) nature-type population mean values in different ratios; (**e**) the land use GDP mean values in different ratios.

In Table 7, W is the correlation coefficient between the LCZ area ratio and the average LST, M is the correlation coefficient between the LCZ area ratio and the average population, and G is the correlation coefficient between the LCZ area ratio and the average GDP.

As shown in the results, for open-type buildings (LCZ4, LCZ5, LCZ6), large low-rise buildings (LCZ8), dense trees (LCZ11), sparse trees (LCZ12), bush and scrub (LCZ13), low plants (LCZ14), and water (LCZ17), the percentages of LCZ areas in these categories were inversely proportional to the LST, because these LCZ types had some vegetation and greenery and were well ventilated, which had a cooling effect on the ground surface. The cooling effect of water bodies (LCZ17) was the most obvious in the natural-cover types, and the cooling effect of open low-rise buildings (LCZ6) was the most obvious in the building types. Except for large low-rise buildings (LCZ8) and natural-cover types (LCZ11–LCZ17), the percentage of LCZ area in all built-up types was proportional to the population number, because built-up types provide the main places for human habitation, living, and production, with compact high-rise buildings (LCZ1) having the most significant effect on population growth. The area ratios of all types of land types were proportional to GDP, except for water (LCZ17). The built-up types (LCZ1–LCZ10) had the most significant effect on GDP. This was because the built-up types were the main places for human activities and production activities, and economic activities were prosperous and contributed to economic development.

From the correlation analysis, we could determine that the number of different LCZs have different impacts on LST, population, and GDP. In the optimization, the impact of each type on different factors should be considered comprehensively, balancing the contradictions between different factors to ensure the environmental, population carrying capacity, and economic development of the city while achieving the optimization goal.

4.2. LCZ Optimization Results

4.2.1. Optimization Results of LCZ Area Proportions

The optimization of the LCZ number structure of Changsha under the appropriate temperature scenario was obtained using a genetic algorithm (Table 8), and the optimized LST was 25.05 °C, which was in line with the human comfort temperature. Accordingly, the LCZ optimization results achieved a −5.2 °C reduction from the maximum average LST of 30.25 °C in Changsha. In Table 8, except for compact high-rise buildings (LCZ1) and heavy industries (LCZ10), the area of LCZs of all built-up types increased, and the increase in open buildings was more than that of compact buildings, the number of open low-rise buildings (LCZ6) increased the most, with an increase of 709.07 km^2, and the proportion of total area increased from 7.78% to 13.76%. Except for bush and scrub (LCZ13) and water (LCZ17), all natural-cover types decreased, and dense trees (LCZ11) decreased the most, namely, by 906.4 km^2, and from 43.85% to 36.21% of the total area. The area of water (LCZ17) increased by 157.77 km^2, and the proportion of total area increased from 1.27% to 2.60%.

Figure 6 shows the LCZ area-transfer Sankey image before and after optimization, where "Be" represents all types of LCZs before optimization, and "Af" represents all types of LCZs after optimization. The lines of different colors represent the changes in the area ratios of different types of LCZs, and the widths of the lines represent the area ratios of LCZs. The conversion relationship between different LCZs can be seen from the figure: sparse buildings (LCZ9) were mainly converted into open low-level buildings (LCZ6), dense trees (LCZ11), scattered trees (LCZ12), and low plants (LCZ14). Furthermore, dense trees (LCZ11) were mainly converted into sparse buildings (LCZ9) and then converted into scattered trees (LCZ12). The optimized open low-rise buildings (LCZ6) were mostly transferred from sparse buildings (LCZ9) and dense trees (LCZ11), while sparse buildings (LCZ9) were mostly transferred from dense trees (LCZ11) and low vegetation (LCZ14). The optimization of the quantitative structure was overall consistent with the policy of building an eco-tourism city in Changsha.

Table 8. The quantity optimization results of Changsha in 2020.

LCZs	Area before Optimization (km^2)	Ratio before Optimization	Area after Optimization (km^2)	Ratio after Optimization	Change Area (km^2)
LCZ1 Compact high-rise	5.29	0.04%	3.52	0.03%	−1.77
LCZ2 Compact high-rise	16.06	0.14%	30.43	0.26%	+14.36
LCZ3 Compact high-rise	22.77	0.19%	45.93	0.39%	+23.16
LCZ4 Open high-rise	75.43	0.64%	76.51	0.65%	+1.08
LCZ5 Open high-rise	85.73	0.72%	147.97	1.25%	+62.25
LCZ6 Open low-rise	922.36	7.78%	1631.43	13.76%	+709.07
LCZ8 Large low-rise	428.92	3.62%	508.84	4.29%	+79.92
LCZ9 Sparsely built	3428.73	28.93%	3602.66	30.40%	+173.93
LCZ10 Heavy industries	3.29	0.03%	1.48	0.01%	−1.80
LCZ11 Dense trees	5197.61	43.85%	4291.21	36.21%	−906.40
LCZ12 Scattered trees	709.92	5.99%	643.03	5.43%	−66.89
LCZ13 Scattered trees	0.18	0.002%	0.63	0.01%	+0.45
LCZ14 Low plants	789.86	6.66%	556.35	4.69%	−233.51
LCZ15 Bare rock or paved	4.64	0.04%	1.20	0.01%	−3.44
LCZ16 Bare soil or sand	11.47	0.10%	3.29	0.03%	−8.18
LCZ17 Water	149.98	1.27%	307.75	2.60%	+157.77

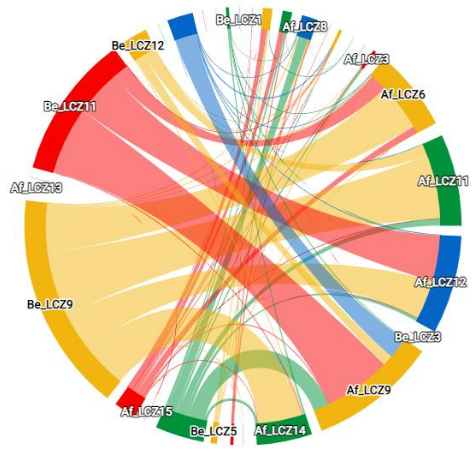

Figure 6. Sankey diagram before and after local climate zone area optimization.

Combined with the correlation analysis, it could be seen that increasing the natural-cover type can effectively reduce the urban LST, but the population and the average GDP will also decrease significantly, so it was undesirable to increase the natural-cover type. In our proposed optimization scheme, we added a large number of open low-rise buildings (LCZ6) to reduce the LST. Combined with the correlation analysis results, the number of this type was inversely proportional to the LST, and increasing this type could reduce the LST, and it was the most obvious cooling effect among the built-up types. We also increased the area of water (LCZ17) because the correlation analysis showed that water (LCZ17) was the most effective in reducing urban LST among the natural-cover types. The number of open low-rise buildings (LCZ6) was also proportional to the number of population and GDP, so increasing this type can promote the growth of population and GDP while reducing the LST, which was consistent with our optimization objectives. Although the number of compact high-rise buildings (LCZ1) was highly positively correlated with population and GDP, which could attract population to promote economic development, the high positive correlation between its number and LST could also lead to a dramatic increase in LST and intensify the urban heat island effect, so our optimization scheme did not add this category. Our optimization scheme optimized the urban LST under the premise of ensuring economic development, population carrying capacity, and relevant policies, given priority to ecology while taking into account social development, and therefore it had a certain degree of rationality. The results of this optimization could be used as constraints for the subsequent spatial layout optimization of LCZs.

4.2.2. Optimization Results of Spatial LCZ Layout

In this paper, based on the 2020 LCZ map, we optimized the spatial layout of LCZs under the control of the LCZ number in Changsha and the conversion rules (Figure 7). The LCZ spatial layout optimization results showed that urban expansion was mainly concentrated in the central area of Changsha, and natural cover such as forest vegetation was still commonly distributed in the eastern part of Changsha. The open low-rise buildings (LCZ6) type was mainly increased in the center of the city, connecting with the existing buildings, while the compact high-rise buildings (LCZ1) type was reduced. The NingXiang area in the west added many open low-rise buildings (LCZ6) and some low plants (LCZ14). The LiuYang area in the east saw a decrease in the overall area of forest vegetation, converting it mainly to open low-rise buildings (LCZ6) and sparse buildings (LCZ9).

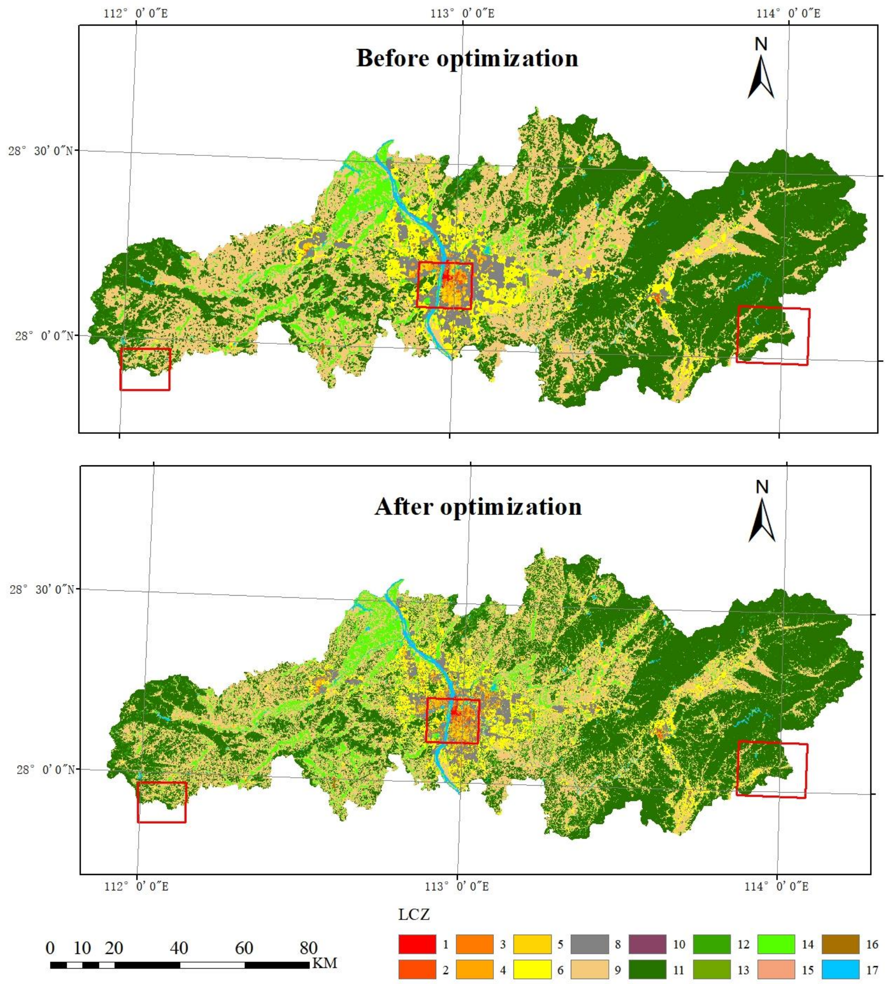

Figure 7. Optimization results of local climate zones in Changsha in 2020.

Figure 8 shows the details of optimization. It can be seen that in the center of the city, large low-rise buildings (LCZ8) were converted to open-type buildings (including open high-rise, open mid-rise, and open low-rise), and these open-type buildings expanded outward from the original buildings. The increase in open-type buildings ensured the economic development and population-carrying ability without ignoring the greenery, which contributed to the reduction of urban LST. In addition, the compact high-rise buildings (LCZ1) remained unchanged, because the renovation cost of this type was high, and it was mostly new construction, which was not suitable for renovation. There was also an increasing trend of low plants (LCZ14) in the city, and the increase in this class was also beneficial for improving the urban heat environment. In the eastern part of the city (LiuYang), dense trees (LCZ11) were converted to sparse buildings (LCZ9), and the increase in this type could reduce the population pressure in the city center and promote the economic development of eastern LiuYang, while ensuring that the forest cover would not be reduced too much. The western part of the city (NingXiang) was converted from sparse buildings (LCZ9) to open low-rise buildings (LCZ6) with an accompanying increase in low plants (LCZ14). The simultaneous increase in these two LCZ types helped both the development of tertiary industry and the maximum natural environment in NingXiang and helped to reduce the LST while ensuring the economic development. All regional water (LCZ17) was effectively protected and increased to a certain extent, which helped to alleviate the urban thermal environment and build a city with a livable temperature.

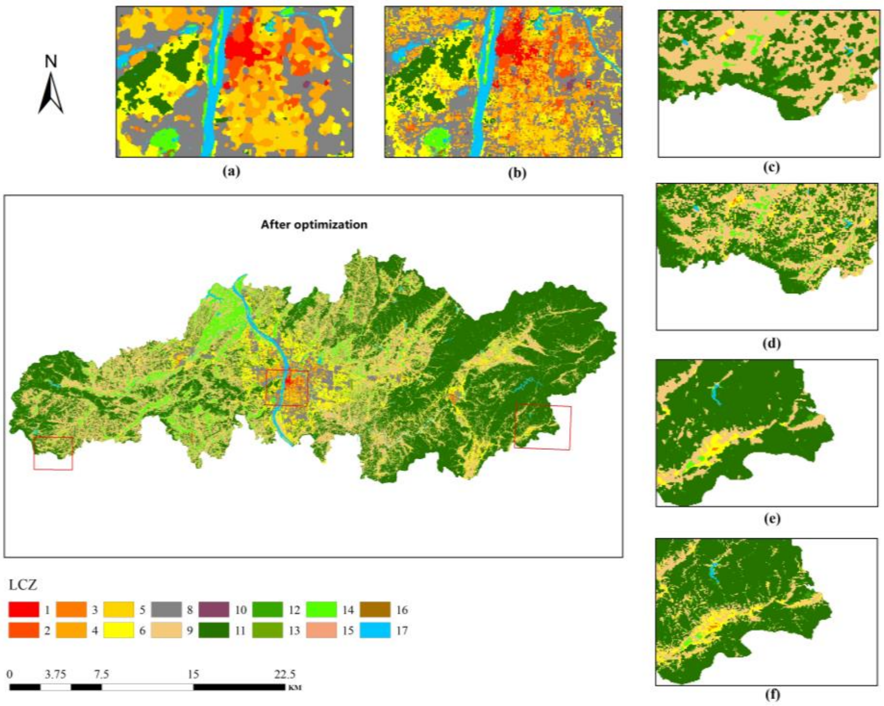

Figure 8. Optimization details of local climate zones in Changsha in 2020. (**a**) The local climate zones before optimization in central Changsha; (**b**) the local climate zones after optimization in central Changsha; (**c**) the local climate zones before optimization in western Changsha; (**d**) the local climate zones after optimization in western Changsha; (**e**) the local climate zones before optimization in eastern Changsha; (**f**) the local climate zones after optimization in eastern Changsha.

In summary, the spatial layout optimization of LCZs under the consideration of the constraint of the number of LCZs and the conversion rules was consistent with the development plan of Changsha, namely, to build the core area of the city center and the sub-centers of NingXiang and LiuYang, two administrative districts far away from the city center, and helping to promote the development of urban clusters, form an integrated urban–rural development pattern, and optimize the urban environment and help to build a modernized new city.

Based on the optimization results, we suggested that the future urban construction of Changsha should consider the central city and the surrounding townships simultaneously. In eastern LiuYang, open low-rise buildings (LCZ6) should be formed by constructing beautiful environments such as advanced residential districts or farmhouses. In western NingXiang, the sparse buildings (LCZ9) such as hot spring towns should be built to construct a combined urban–rural development corridor. The construction of the city center should be mainly renovated, expanding outward along the basis of the original buildings and building open low-rise buildings (LCZ6).

4.3. Discussion

Guided by the sustainability of human life and based on the correlation between LCZs and climate and socioeconomic datasets, this study constructed a GA-FLUS model to optimize the LCZs in Changsha City. The area proportions optimization results showed that open low-rise buildings (LCZ6) increased the most, with an increase of 709.07 km^2, which was mainly converted from sparse buildings (LCZ9) and dense trees (LCZ11). Furthermore, dense trees (LCZ11) decreased the most, namely, by 906.4 km^2, which was mainly converted to sparse buildings (LCZ9) and scattered trees (LCZ12). The results of spatial layout optimization showed that open low-rise buildings (LCZ6) mainly increased around existing buildings in the center of the city, while dense trees (LCZ11) decreased a lot in the east and west areas. Not only the layout of the city center was changed, as the east and west of city were built at the same time.

In order to discuss the significance of the optimization results for urban planning, we compared the results to Changsha's 2003–2020 urban planning scheme. According to the planning, the core development area was in the central urban area of Changsha from 2003 to 2020. In addition, two secondary planning centers (downtown LiuYang and downtown NingXiang) were horizontal development to the east and west and vertically integrated development relying on the Xiangjiang River. Combined with the optimized results (Figure 7), the open low-rise buildings (LCZ4) increased in the central urban area of Changsha, while a large number of dense trees (LCZ11) in the eastern LiuYang and the western NingXiang were converted to open low-rise buildings (LCZ4). It can be seen that overall, Changsha's planning development direction was consistent with our optimization results, and the results of LCZ spatial-layout optimization in this paper were confirmed in the urban planning scheme.

According to the general land-use planning map of Changsha, the planning of the central city focused on the existing CBD and expanding residential and commercial land use, and it promoted north–south public service construction, ensuring the original wetland resources, and established a green corridor along the Xiangjiang River. This development plan matched our urban center optimization results (Figure 8b), i.e., the new building type LCZs were centered on the original building type LCZs with a north–south vertical layout and a large number of natural-cover LCZ types distributed along the Xiangjiang River. In addition, the plan showed that in addition to construction in the central urban area, two sub-city centers in LiuYang and NingXiang in the east and west would be built at the same time. In eastern Changsha, LiuYangis is centered on the county town, while the development areas are built in several towns based on the superior natural environment, focused on strengthening the ecological protection and construction of areas such as the LiuYang River, the Lianyun Mountain, and the Dawei Mountain. In the optimization results of Wenjiashi Town in LiuYang (Figure 8d), many new sparse buildings (LCZ9) had been added, and this type was usually accompanied by natural-cover types. The planning goal of LiuYang, which places equal emphasis on ecological protection and development, coincided with our optimization results (Figure 8d). In the planning and construction, the spatial development of NingXiang was based on the concept of "developing the central east and protecting the west", and the construction of towns was also arranged around the county town, based on the old city and mainly to the north, with appropriate construction to the east and south, and to develop tertiary industry. The optimization results of the town's development plan, NingXiang Tangshan Town, match Figure 8f, with open low-rise buildings (LCZ6) and low plants (LCZ14) replacing sparse buildings (LCZ9). The planning goal of developing tertiary industry in NingXiang based on the local natural resource environment matched our optimization results (Figure 8f). Figure 9a shows that the proportion of agricultural land in Changsha at the end of the planning period (2020) decreased by 4 percentage points, the proportion of building land increased by 5 percentage points, and the proportion of other land did not change significantly. The LCZ optimization results (Figure 9b) showed that the proportion of LCZs of vegetation of the natural-cover type decreased by 10 percentage points after optimization, the proportion of LCZs of the building type increased by nearly 9 percentage points, and the proportion of LCZs of other natural-cover type increased by slightly more than 1 percentage point. The LCZ optimization results were generally consistent with the planning results.

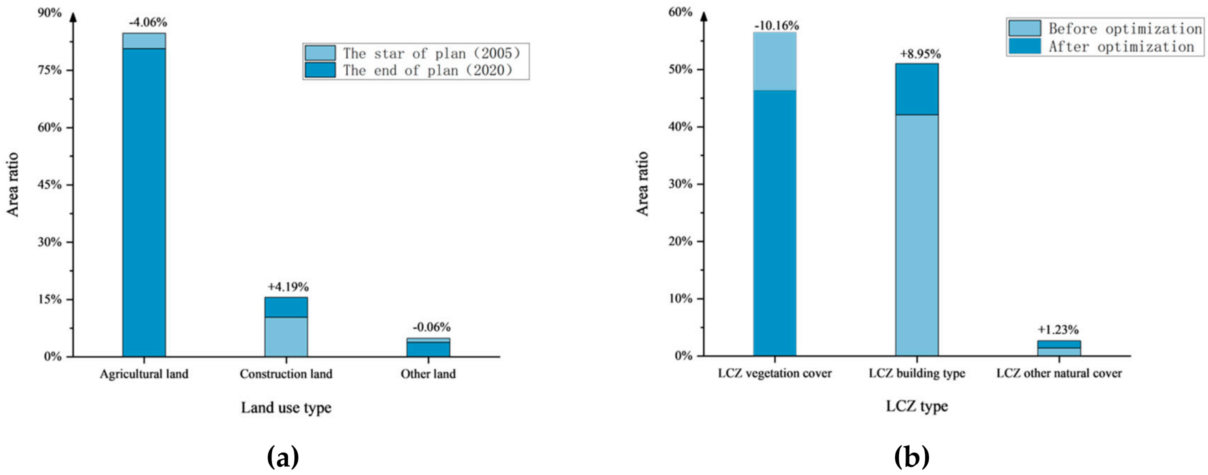

Figure 9. Comparison between planning and optimization. (**a**) Area ratio of each land type before and after plan in Changsha; (**b**) area ratio of each local climate zones type before and after optimization in Changsha.

In practical application, according to the results, quantity optimization could guide the overall direction of urban planning and design and determine the types which need to be increased and reduced. According to the results of spatial layout optimization, the area where urban planning and design was specifically implemented, and the area that should be focused on in urban planning and construction could be detected. The optimization results of this paper showed that the urban planning of Changsha City should increase the types of open buildings and reduce the amount of dense forests. Urban planning should consider both the city center and the surrounding towns and strive for multi-point development.

In general, our optimization results were generally consistent with existing urban planning in Changsha. Therefore, our optimization results could not only provide solutions for building a city with livable temperatures but also reflect the development direction of the city and provide references and suggestions for urban planning.

5. Conclusions and Limitations

5.1. Conclusions

This paper aimed to optimize the urban thermal environment without losing population carrying capacity and economic development. In this paper, the spatial LCZ layout in Changsha was optimized by identifying the LCZs and modeling the correlations between LCZs and urban LST, population, and economic level. It was found that the rapid economic development of Changsha, the surge in population, and the large number of buildings led to the increase in LST, affecting the urban heat environment and livability.

We used the GA-FLUS model to optimize the 3D LULC LST. Under the constraints of water area, forest and grass coverage, population carrying capacity, social economy, and land area, the optimization result could protect the ecological environment, ensure social development, reduce the LST, and improve the urban heat environment in Changsha.

For the optimization result, the area of all built types increased, except dense high-rise buildings (LCZ1) and heavy industries (LCZ10). Furthermore, the open low-rise buildings (LCZ6) increased the most, by 699.07 km^2. The area of all natural-cover types decreased except water (LCZ17) and bush and shrubs (LCZ13), with dense trees (LCZ11) decreasing the most, namely, by 906.4 km^2. Furthermore, 62.97% of open low-rise buildings (LCZ6) were transformed from sparse buildings (LCZ9), and 22.34% were transformed from dense trees (LCZ11); this change reduced the LST and ensured the city's population and economic development. As for spatial layout optimization, some open buildings (including open high-rise, open mid-rise, and open low-rise) were added to the urban center, while low plants (LCZ14) were added. In the eastern LiuYang and the western NingXiang, open low-rise buildings (LCZ6) were added, while dense trees (LCZ11) were reduced, which was the same as the planning goal of "one urban center and two sub-centers" in Changsha. In addition, we also discussed the role of the optimization results in guiding urban planning, and since the Changsha plan matched our optimization results to some extent, our optimized structure can provide a reference and suggestions for urban planning.

5.2. Limitations and Future Research

There were still some deficiencies in this paper; in particular, there were still many uncertainties in LCZs and many nonlinear problems in the optimization of quantity structures. In addition, this paper did not consider the influence of the landscape pattern of LCZs within 1×1 km on the temperature, population, and economy, and although the 1×1 km grid avoided the rough analysis scale at an administrative division scale, each grid still had more than one LCZ. These problems caused some limitations in spatial layout optimization. Furthermore, the LCZ conversion cost matrix (Table 4) was set according to Balling's research [44,45]. The matrix illustrated the difficulty of the LCZs and the watershed protection and forest land protection policies, which was applicable to most cities. However, for the special situation of each city, the setting of the conversion cost matrix needs further consideration. The low resolution of the available data used in this paper could have had an impact on the results. Data quality and data uniformity are meaningful factors for future research.

Therefore, in future research, nonlinear programming must be considered to improve the accuracy of the optimization model, so that the model optimization results are closer to reality. In spatial layout optimization, a finer spatial analysis grid could be considered to analyze the correlation between LCZs and climate and socioeconomic data, and a landscape pattern index could be added to consider the influence of the landscape pattern of LCZs on social development and economic development to make the spatial layout optimization more credible. When setting the LCZ conversion cost matrix, the actual situation of urban development and government planning requirements should be considering, so that the optimization results can be more realistic. We know that there are great uncertainties and policy orientations for LULC optimization, and the development goals of each region are different [36]. We can construct different land-use change simulation scenarios to adapt to the multiple possibilities of regional development in subsequent research. With the increased interest in research on sustainable urban development, there is a lot of data available. In future research, higher resolution data should be selected, and more attention should be paid to harmonization between data.

Author Contributions: Conceptualization, J.C. and X.Z.; Data curation, R.S.; Formal analysis, R.S.; Funding acquisition, J.C. and M.D.; Investigation, R.S. and G.S.; Methodology, R.S. and Y.G.; Project administration, M.D.; Resources, M.D.; Software, G.S.; Supervision, J.C.; Validation, G.S. and Y.G.; Visualization, R.S.; Writing—original draft, R.S.; Writing—review and editing, J.C. and X.Z. All authors have read and agreed to the published version of the manuscript.

Funding: This research was funded in part by the National Natural Science Foundation of China, grant 42071427, and in part by the Central South University Research Program of Advanced Interdisciplinary Studies, grant 2023QYJC033.

Institutional Review Board Statement: Not applicable.

Informed Consent Statement: Not applicable.

Data Availability Statement: Data are contained within the article.

Conflicts of Interest: The authors declare no conflict of interest.

References

1. United Nations. Transforming Our World: The 2030 Agenda for Sustainable Development. 2015. Available online: https://sdgs.un.org/2030agenda (accessed on 14 April 2023).
2. United Nations. *The Sustainable Development Goals Report 2018*; United Nations Publications: New York, NY, USA, 2018.
3. Hou, K.; Wen, J. Quantitative analysis of the relationship between land use and urbanization development in typical arid areas. *Environ. Sci. Pollut. Res.* **2020**, *27*, 38758–38768. [CrossRef] [PubMed]
4. Zhao, T.L.; Miao, L.; Bei, C.X. Spatio-temporal dynamics of ecological security pattern of the Pearl River Delta urban agglomeration based on LUCC simulation. *Ecol. Indic.* **2023**, *114*, 106319. [CrossRef]
5. Zou, L.; Liu, Y.; Wang, J.; Yang, Y.; Wang, Y. Land use conflict identification and sustainable development scenario Simulation on China's southeast coast. *J. Clean. Prod.* **2019**, *238*, 117899.1–117899.16. [CrossRef]
6. Gries, T.; Redlin, M.; Ugarte, J.E. Human-induced climate change: The impact of land-use change. *Theor. Appl. Climatol.* **2019**, *135*, 1031–1044. [CrossRef]
7. Li, C.; Wu, K.; Wu, J. Urban land use change and its socio-economic driving forces in China: A case study in Beijing, Tianjin and Hebei region. *Environ. Dev. Sustain.* **2018**, *20*, 1405–1419. [CrossRef]
8. Yin, Y.; Pierce, J.T.; Love, E. Designing a Multisector Model for Land Conversion Study. *J. Environ. Manag.* **1995**, *44*, 249–266. [CrossRef]
9. Li, X.; Anthony, G.Y. Modelling sustainable urban development by the integration of constrained cellular automata and GIS. *Int. J. Geogr. Inf. Sci.* **2000**, *14*, 131–152. [CrossRef]
10. Liu, Y.L.; Liu, D.F.; Liu, Y.F. Rural land use spatial allocation in the semiarid loess hilly area in China: Using a particle swarm optimization model equipped with multi-objective optimization techniques. *Sci. China (Earth Sci.)* **2012**, *55*, 1166–1177. [CrossRef]
11. Shen, Q.; Chen, Q.; Tang, B. A system dynamics model for the sustainable land use planning and development. *Habitat Int.* **2008**, *33*, 15–25. [CrossRef]
12. Opinions of the Central Committee of the Communist Party of China and the State Council on the Key Efforts to Comprehensively Promote Rural Revitalization in 2022. Available online: https://www.gov.cn/zhengce/2022-02/22/content_5675035.htm (accessed on 14 April 2023).
13. Cao, K.; Huang, B.; Wang, S.W. Sustainable land use optimization using boundary-based fast genetic algorithm. *Comput. Environ. Urban Syst.* **2011**, *36*, 257–269. [CrossRef]
14. Wang, X.; Yao, Y.; Ren, S. A Coupled FLUS and Markov approach to simulate the spatial pattern of land use in rapidly developing cities. *J. Geo-Inf. Sci.* **2022**, *24*, 100–113.
15. Li, X.; Fu, J.Y.; Jiang, D. Land use optimization in Ningbo city with a coupled GA and PLUS model. *J. Clean. Prod.* **2022**, *375*, 134004. [CrossRef]
16. Yang, Y.; Bao, W.K.; Liu, Y.S. Scenario simulation of land system change in the Beijing-Tianjin-Hebei region. *Land Use Policy* **2020**, *96*, 104677. [CrossRef]
17. Liu, X.P.; Liang, X.; Li, X. A future land use simulation model (FLUS) for simulating multiple land use scenarios by coupling human and natural effects. *Landsc. Urban Plan.* **2017**, *168*, 94–116. [CrossRef]
18. Han, J.; Hu, Z.; Wang, P.; Yan, Z.; Li, G.; Zhang, Y.; Zhou, T. Spatio-temporal evolution and optimization analysis of ecosystem service value—A case study of coal resource-based city group in Shandong, China. *J. Clean. Prod.* **2022**, *363*, 132602. [CrossRef]
19. Xu, Z.; Chau, S.N.; Chen, X.Z. Assessing progress towards sustainable development over space and time. *Nature* **2020**, *577*, 74–78. [CrossRef]
20. Lu, X.H.; Zhang, Y.W.; Lin, C.Y. Analysis and comprehensive evaluation of sustainable land use in China: Based on sustainable development goals framework. *J. Clean. Prod.* **2021**, *310*, 127205. [CrossRef]
21. Liao, T.; Li, D.; Wan, Q. Trade off of exploitation-protection and suitability evaluation of low-slope hilly from the perspective of "production-living-ecological" optimization. *Phys. Chem. Earth Parts A/B/C* **2020**, *120*, 102943. [CrossRef]
22. Tian, F.H.; Li, M.Y.; Han, X.L. A production–living–ecological space model for land-use optimization: A case study of the core Tumen River region in China. *Ecol. Model.* **2020**, *437*, 109310. [CrossRef]
23. Wang, H.T.; Zheng, S.X.; Wang, Y.C. Research progress on the evolution of production-life-ecological spatial pattern and its analytical techniques. *J. Jinan Univ. (Nat. Sci. Ed.)* **2022**, *36*, 462–469.
24. Li, S. Spatiotemporal Characteristics of the Surface Urban Heat Island and Its Driving Factors Based on Local Climate Zones and Population in Beijing, China. *Atmosphere* **2021**, *12*, 271. [CrossRef]
25. Stewart, I.D.; Oke, T.R. Local climate zones for urban temperature studies. *Bull. Am. Meteorol. Soc.* **2012**, *93*, 1879–1900. [CrossRef]
26. Geletič, J.; Lehnert, M.; Dobrovolný, P. Land surface temperature differences within local climate zones, based on two central European cities. *Remote Sens.* **2016**, *8*, 788–806. [CrossRef]
27. Marie, V.; Matthias, D.; Hans, H. The potential of local climate zones maps as a heat stress assessment tool, supported by simulated air temperature data. *Landsc. Urban Plan.* **2018**, *178*, 183–197.
28. Pereira, C.T.; Masiero, E.; Bourscheidt, V. Socio-spatial inequality and its relationship to thermal (dis)comfort in two major Local Climate Zones in a tropical coastal city. *Int. J. Biometeorol.* **2021**, *65*, 1177–1187. [CrossRef] [PubMed]

29. Ching, J.; Mills, G.; Bechtel, B. World Urban Database and Access Portal Tools (WUDAPT), an urban weather, climate and environmental modeling infrastructure for the Anthropocene. *Bull. Am. Meteorol. Soc.* **2018**, *99*. [CrossRef]
30. Mills, G.; Ching, J.; See, L.; Bechtel, B.; Foley, M. An introduction to the WUDAPT project. In Proceedings of the 9th International Conference on Urban Climate, Toulouse, France, 20–24 July 2015; pp. 20–24.
31. Lau, K.K.L.; Chung, S.C.; Ren, C. Outdoor thermal comfort in different urban settings of sub-tropical high-density cities: An approach of adopting local climate zone (LCZ) classification. *Build. Environ.* **2019**, *154*, 227–238. [CrossRef]
32. Liu, L.; Lin, Y.; Xiao, Y.; Xue, P.; Shi, L.; Chen, X.; Liu, J. Quantitative effects of urban spatial characteristics on outdoor thermal comfort based on the LCZ scheme. *Build. Environ.* **2018**, *143*, 443–460. [CrossRef]
33. Wu, Y.; Sharifi, A.; Yang, P.; Borjigin, H.; Murakami, D.; Yamagata, Y. Mapping building carbon emissions within local climate zones in Shanghai. *Energy Procedia* **2018**, *152*, 815–822. [CrossRef]
34. Järvi, L.; Havu, M.; Ward, H.C.; Bellucco, V.; McFadden, J.P.; Toivonen, T.; Heikinheimo, V.; Kolari, P.; Riikonen, A.; Grimmond, C.S.B. Spatial Modeling of Local-Scale Biogenic and Anthropogenic Carbon Dioxide Emissions in Helsinki. *J. Geophys. Res. Atmos.* **2019**, *124*, 8363–8384. [CrossRef]
35. Statistical Yearbook of Urban Construction. Ministry of Housing and Construction, 2010–2020. Available online: https://www.mohurd.gov.cn/ (accessed on 9 March 2023).
36. Rahman, M.M.; Szabó, G. Multi-objective Urban Land Use Optimization using Spatial Data: A Systematic Review. *Sustain. Cities Soc.* **2021**, *74*, 103214. [CrossRef]
37. Song, M.; Chen, D. A comparison of three heuristic optimization algorithms for solving the multi-objective land allocation (MOLA) problem. *Ann. GIS* **2018**, *24*, 19–31. [CrossRef]
38. Zeng, X.; Zhan, L.; Luo, C.W. A Study on Optimization Method of Green Landscape Pattern Around Environment Based on Ca-Markov Model. *Fresenius Environ. Bull.* **2022**, *31*, 1610–2304.
39. Schweitzer, C.; Priess, J.A.; Das, S. A generic framework for land-use modelling. *Environ. Model. Softw.* **2011**, *26*, 1052–1055. [CrossRef]
40. Leta, M.K.; Demissie, T.A.; Trnckner, J. Modeling and Prediction of Land Use Land Cover Change Dynamics Based on Land Change Modeler (LCM) in Nashe Watershed, Upper Blue Nile Basin, Ethiopia. *Sustainability* **2021**, *13*, 3740. [CrossRef]
41. Zhao, X.; Calvin, K.V.; Wise, M.A. The Critical Role of Conversion Cost and Comparative Advantage in Modeling Agricultural Land Use Change. *Clim. Change Econ. (CCE)* **2020**, *11*, 1–44. [CrossRef]
42. Hu, S.; Chen, L.Q.; Li, L.; Zhang, T. Simulation of Land Use Change and Ecosystem Service Value Dynamics under Ecological Constraints in Anhui Province, China. *Int. J. Environ. Res. Public Health* **2020**, *17*, 4228. [CrossRef]
43. Xu, Q.; Guo, P.; Jin, M.T.; Qi, J.F. Multi-scenario landscape ecological risk assessment based on Markov-FLUS composite model. *Geomat. Nat. Hazards Risk* **2021**, *12*, 1449–1466. [CrossRef]
44. Richard, B.; Brent, P.; Mitsuro, S. Generating future land-use and transportation plans for high-growth cities using a genetic algorithm. *Comput. Aided Civ. Infrastruct. Eng.* **2004**, *19*, 213–222.
45. Liu, X.Q.; Huang, B.; Du, S.S.; Yan, X.X. A multi-objective optimization method for land use space in ecologically livable cities. *Geogr. Inf. World* **2019**, *26*, 7.